

Electronic Supplementary Information

Dopant-free hole-transporting materials for $\text{Sb}_2(\text{S,Se})_3$ solar cells enabling enhanced stability

Yinan Xiang,^{‡a} Huanxin Guo,^{‡b} Zhiyuan Cai,^a Chenhui Jiang,^a Changfei Zhu,^a Yongzhen Wu,^{*b} Wei-Hong Zhu^b and Tao Chen^{*a}

[a] Hefei National Laboratory for Physical Sciences at Microscale, Department of Materials Science and Engineering, University of Science and Technology of China, No. 96 Jinzhai Road, Hefei, Anhui Province, 230026, P. R. China.

*E-mail: tchenmse@ustc.edu.cn (T. C)

[b] Institute of Fine Chemicals, East China University of Science and Technology, Meilong Road 130, Shanghai 200237, P. R. China.

*E-mail: wu.yongzhen@ecust.edu.cn (Y. W)

Device Fabrication

Before CdS deposition, the FTO-coated glass was ultrasonic cleaned in deionized water, acetone, and ethanol for 40 min, respectively. After drying, the substrate was treated by UV ozone cleaner for 15 min. Then, CdS electron transport layer was deposited by chemical bath deposition at 65 °C for 15 minutes on the substrate with thickness of about 60 nm, in which $\text{Cd}(\text{NO}_3)_2$ (0.015 mol L^{-1}), thiourea (1.50 mol L^{-1}) and ammonia (1.56 mol L^{-1}) were employed in the precursor solution. After deposition, a post-treatment of CdS by 20 mg mL^{-1} CdCl_2 absolute methanol solution was conducted by spin coating at 3000 r.p.m. for 30 s. Finally, the CdS substrate was annealed in air at 400 °C for 10 min, followed by cooling down to room temperature naturally.

The $\text{Sb}_2(\text{S,Se})_3$ film was deposited by the hydrothermal method. Potassium antimony (III) L(+)- tartrate hemihydrate ($\text{C}_4\text{H}_4\text{KO}_7\text{Sb}\cdot 0.5\text{H}_2\text{O}$), sodium thiosulfate pentahydrate ($\text{Na}_2\text{S}_2\text{O}_3\cdot 5\text{H}_2\text{O}$), and selenourea ($\text{CH}_4\text{N}_2\text{Se}$) were used as Sb, S, and Se sources, respectively. Firstly, 0.2671g $\text{C}_4\text{H}_4\text{KO}_7\text{Sb}\cdot 0.5\text{H}_2\text{O}$ was dissolved in 40 mL deionized water in a Teflon tank (50 mL). Subsequently, $\text{Na}_2\text{S}_2\text{O}_3\cdot 5\text{H}_2\text{O}$ (0.7942 g) and $\text{CH}_4\text{N}_2\text{Se}$ (0.025 g) were added into the solution and stirred until the solution becoming yellow. Afterwards, the CdS layer coated FTO was placed facing down in the growth solution in Teflon tank of an autoclave. The $\text{Sb}_2(\text{S,Se})_3$ film was deposited at 135 °C for 120 min. The obtained $\text{Sb}_2(\text{S,Se})_3$ films were washed with deionized water and ethanol, followed by drying in a N_2 flow in ambient air and baked at 110 °C in a vacuum oven for 1 min. Finally, the films were annealed on a plate at 350 °C for 10 min in a glove box filled with N_2 .

The hole transport materials were synthesized following the previous report.¹ For deposition of hole-transport materials, optimal 5 mg TQ2 and TQ4 were dissolved in 1 mL chlorobenzene and dissolving it thoroughly by ultrasonic. The TQ2 and TQ4 solution was spin-coated onto $\text{Sb}_2(\text{S,Se})_3$ film at 3000 rpm for 30 s, followed by annealing at 105 °C for 10 min. Eventually, the Au film was deposited as the back contact by thermal deposition under a pressure of 5.0×10^{-4} Pa. The active area of the device was defined as 0.04 cm^2 .

Film Characterizations

The optical characteristics of the films were measured with a UV-visible spectrophotometer (SOLID 3700). The surface, cross section morphologies of the samples were examined by SEM (FE-SEM SU 8220). The band energies of $\text{Sb}_2(\text{S,Se})_3$ and HTM films were characterized by XPS (Thermo ESCALAB 250XI). UPS (PHI 5000 Versaprobe III) was implemented to measure the Fermi level and valence band of TQ2 and TQ4 films.

Hole mobility of the HTMs was measured by the space-charge-limited current (SCLC) method with hole only device utilizing the configuration of ITO/PEDOT:PSS/HTM/ MoO_3 /Au.² The TQ2 and TQ4 solution with a concentration of 5mg/mL was spin-coated onto PEDOT: PSS film at 3000 rpm for 30 s, followed by annealing at 105 °C for 10 min. The dark current was recorded by a Keithley 2400 apparatus. The results were fitted to a space charge limited form, based on the following equation:³ □

$$J = 9\mu\epsilon_0\epsilon_r V^2 / 8d^3$$

Where J is the current density, μ is the hole mobility, ϵ_0 is the vacuum permittivity (8.85×10^{-12} F m⁻¹), ϵ_r is the dielectric constant of the material (normally taken to approach 3.5 for organic semiconductors), V is the applied bias, d is the film thickness of the active layer obtained from cross-sectional SEM.

The ultrafast transient absorption (TA) measurements were performed on a pump-probe system (Helios, Ultrafast System) with the maximum time delay of ~8 ns using a motorized optical delay line under ambient conditions. The pump pulses at 400 nm (~250 μW) were delivered by an ultrafast optical parametric amplifier (OPera Solo) excited by a regenerative amplifier (Coherent Astrella, 800 nm, 35 fs, 5 mJ, 1 kHz), seeded with a mode-locked Ti:sapphire oscillator (Coherent Vitara, 800 nm, 80 MHz) and pumped with a LBO laser (Coherent Evolution-50C, 1 kHz system). A small amount of 800 nm femtosecond pulses from the regenerative amplifier were used to pump a sapphire crystal to create a 420-800 nm white light continuum as

probe pulses.

The TA spectra were fitted with *Surface Explorer* software by the convoluted multi-exponential function:

$$\Delta A(t) = e^{-\left(\frac{t-t_0}{t_p}\right)^2} * \sum_{i=1}^N A_i e^{-\frac{t-t_0}{\tau_i}}$$

where t is the probe time delay, t_0 is time zero, $t_p = IRF/(2 \cdot \ln 2)$, IRF is the width of instrument response function (full width half maximum), A_i and τ_i are amplitudes and decay lifetimes, respectively, $*$ is convolution. The minimum number of components N to satisfactorily fit the experimental data is two. The average lifetime τ_{ave} was estimated from the fitting parameters according to the following equation $\tau_{ave} = \sum A_i \tau_i^2 / \sum A_i \tau_i$.

Device Characterizations

The $J-V$ curves were recorded using a Keithley 2400 apparatus under solar-simulated AM 1.5 sunlight (100 mW cm^{-2}) with a standard xenon-lamp-based solar simulator (Oriel Sol 3A, Japan). The device leakage current in the dark state was measured by Keithley 2400 apparatus. The solar simulator illumination intensity was calibrated by a monocrystalline silicon reference cell (Oriel P/N 91150 V, with KG-5 visible color filter) calibrated by the National Renewable Energy Laboratory (NREL). The external quantum efficiency (EQE, Model SPIEQ200) was measured using a single source illumination system (halogen lamp) combined with a monochromator. Electrochemical impedance spectroscopy (EIS) measurements were performed using Zahner Mess System PP211 electrochemical workstation at a bias potential of 0.60 V in dark with the frequency ranging from 100 mHz to 1 MHz. In addition, we investigated the charge recombination kinetics using light intensity-dependent V_{oc} measurement by Zahner Mess System PP211 electrochemical workstation.

Calculation Details

All the structure and electric structure were performed with the density functional theory (DFT) as implemented in the Vienna ab initio simulation package (VASP)^{4, 5}. The projected augmented wave (PAW) pseudopotentials were adopted with a cutoff

energy of 400 eV. For the exchange and correlation functional, the generalized gradient approximation (GGA) in the Perdew-Burke-Ernzerhof (PBE) format was used.

The DFT-D3 correction method of Grimme⁶ for description of dispersion interactions in the whole calculation process. In the bulk structure relaxation, the Brillouin zone was sampled by a (3×3×9) k-points mesh with Gamma point centered. All the atoms and cell parameters were fully relaxed until the atomic forces are less than 0.02 eV Å⁻¹. The TQ2, TQ4 molecules were built according to the structural formula at first, then they were relaxed until the atomic forces are less than 0.05 eV Å⁻¹, and only one Gamma point was considered, because they are two big molecules.

According the XRD pattern, the (130) surface of Sb₂(S,Se)₃ is identified as the dominated surface of absorption layer (Figure S11). So we built the (130) surface to simulate the interface of Sb₂(S,Se)₃/TQ2, Sb₂(S,Se)₃/TQ4. The (130) surface of Sb₂S₃ were built firstly with a 15 Å vacuum thickness added along the Z direction to avoid unnecessary interlayer interactions. Afterwards, we replaced S with Se in the (130) surface of Sb₂S₃ to build the (130) surface of Sb₂(S,Se)₃, there are 200 atoms in one cell. The formula of this cell is Sb₈₀S₉₅Se₂₅, which fits the result of EDS, with the Se/(Se+S) approximately equaling to 0.21. The surface was under full relaxation before we combined it with the molecules of hole transport layer material.

We combined the TQ2 and TQ4 with the surface we built before and the Brillouin zone of them were sampled only by a G point due to the huge volume of supercell. During the process of structural optimization, all the atoms were fully relaxed until the atomic forces are less than 0.05 eV Å⁻¹.

The visualizations of the crystal structure and the charge density were by virtue of the VESTA code.

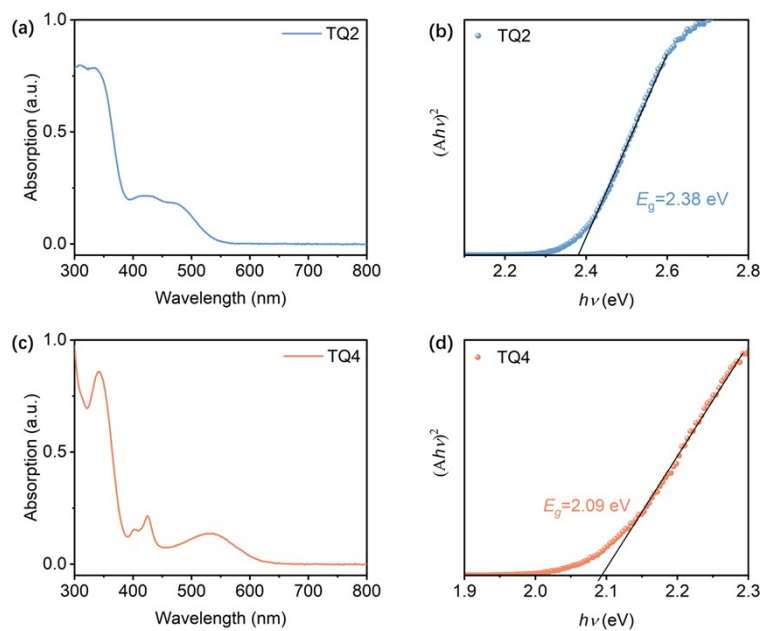


Figure S1 UV-vis absorption spectra of TQ2 (a) and TQ4 (c) films; $(Ah\nu)^2$ vs energy ($h\nu$) curves of TQ2 (b) and TQ4 (d) films.

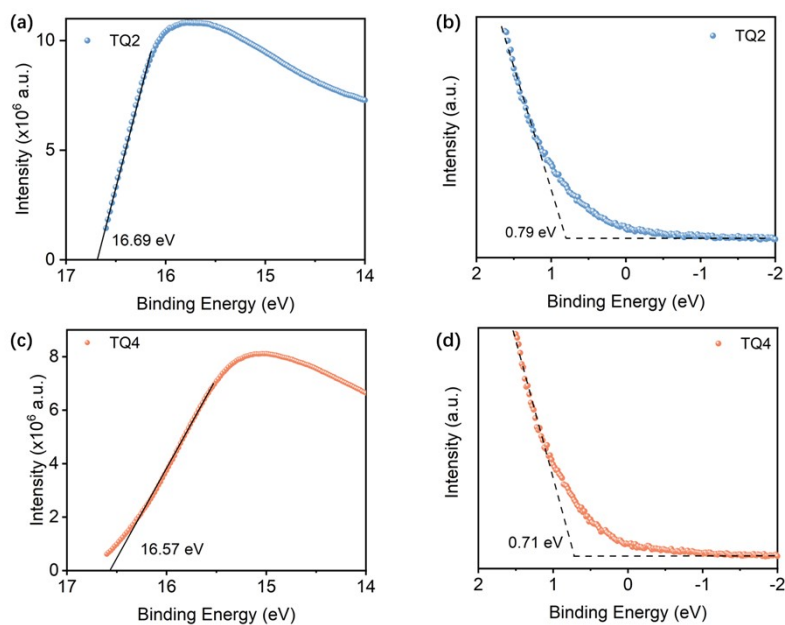


Figure S2 UPS spectra of TQ2 and TQ4 films for a, c) SEC region, b, d) VB region.

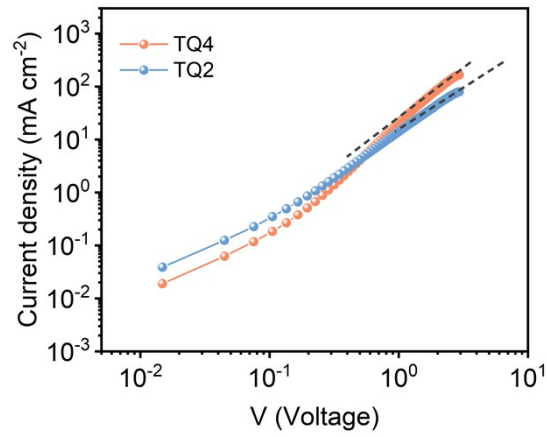


Figure S3 SCLC hole-mobility curves of devices with the structure of ITO/PEDOT:PSS/HTM(ca. 30 nm)/MoO₃/Au.

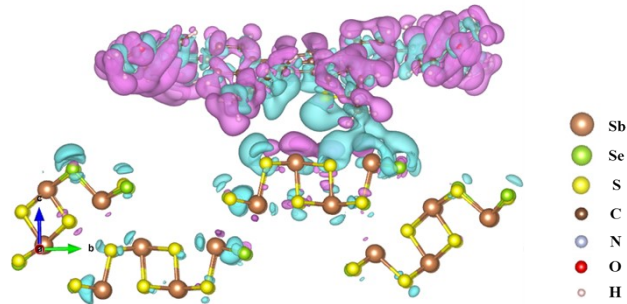


Figure S4 Charge density distribution maps of the Sb₂(S,Se)₃/TQ2 interface.

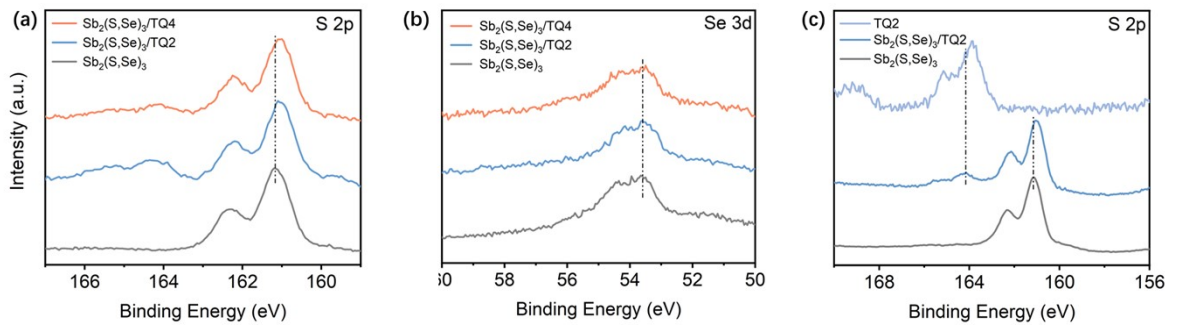


Figure S5 XPS spectra of Sb₂(S,Se)₃, TQ2 and TQ4 films and those deposited on Sb₂(S,Se)₃ films for S,Se element, respectively.

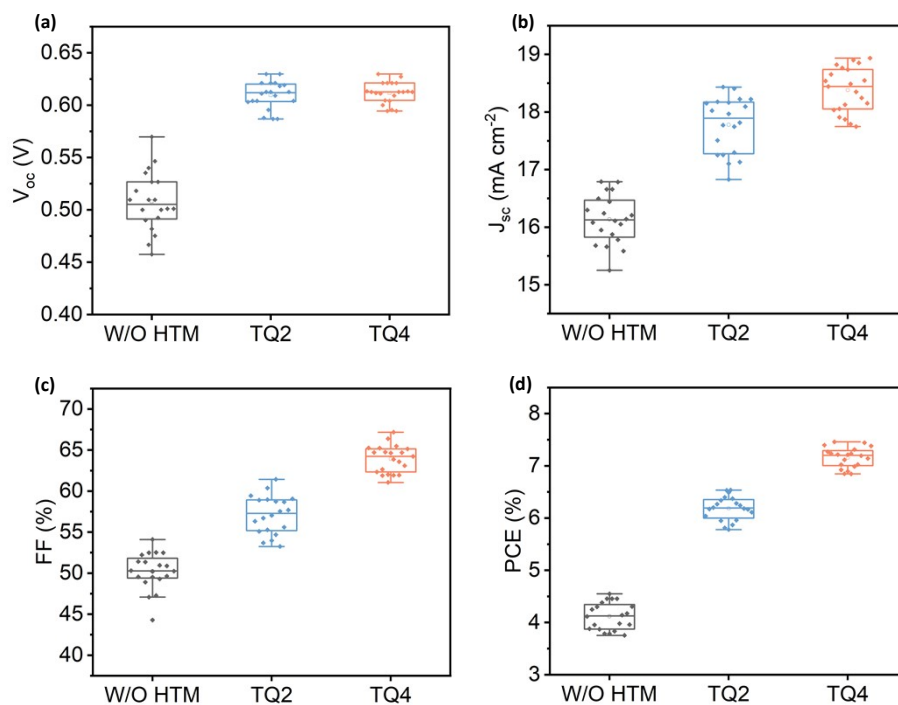


Figure S6 Device performance statistics for $\text{Sb}_2(\text{S,Se})_3$ solar cells with different HTMs (20 individual devices for each batch).

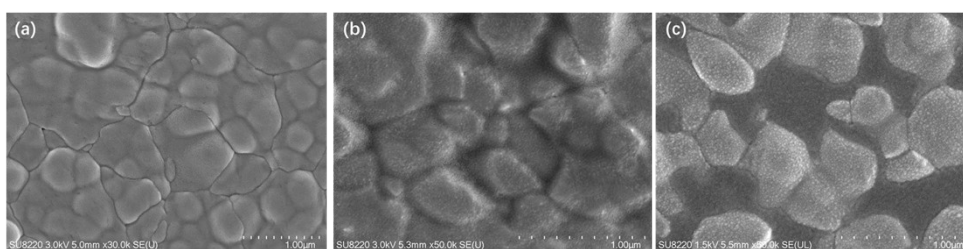


Figure S7 The surface morphologies of (a) $\text{Sb}_2(\text{S,Se})_3$, (b) $\text{Sb}_2(\text{S,Se})_3/\text{TQ4}$ HTM and (c) $\text{Sb}_2(\text{S,Se})_3/\text{TQ2}$ HTM.

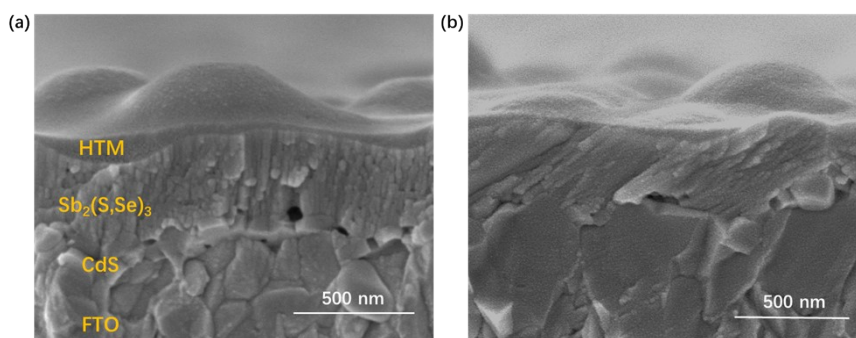


Figure S8 The cross-sectional morphologies of the $\text{Sb}_2(\text{S,Se})_3$ with (a) TQ4 and (b) TQ2 HTM.

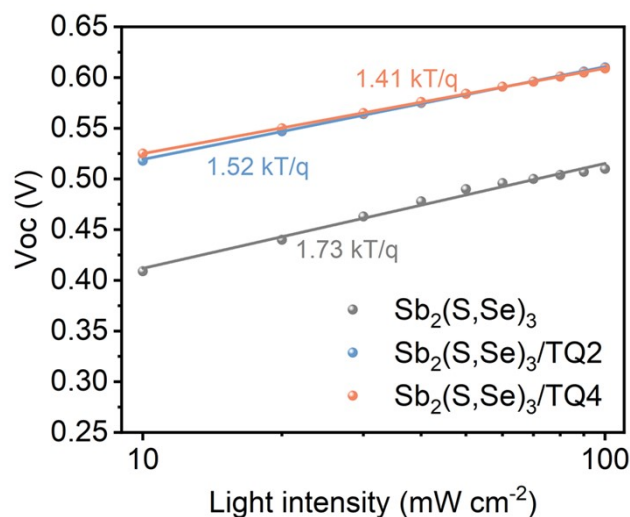


Figure S9 the dependence of V_{oc} on different light intensity for the W/O HTM, TQ2 and TQ4 devices.

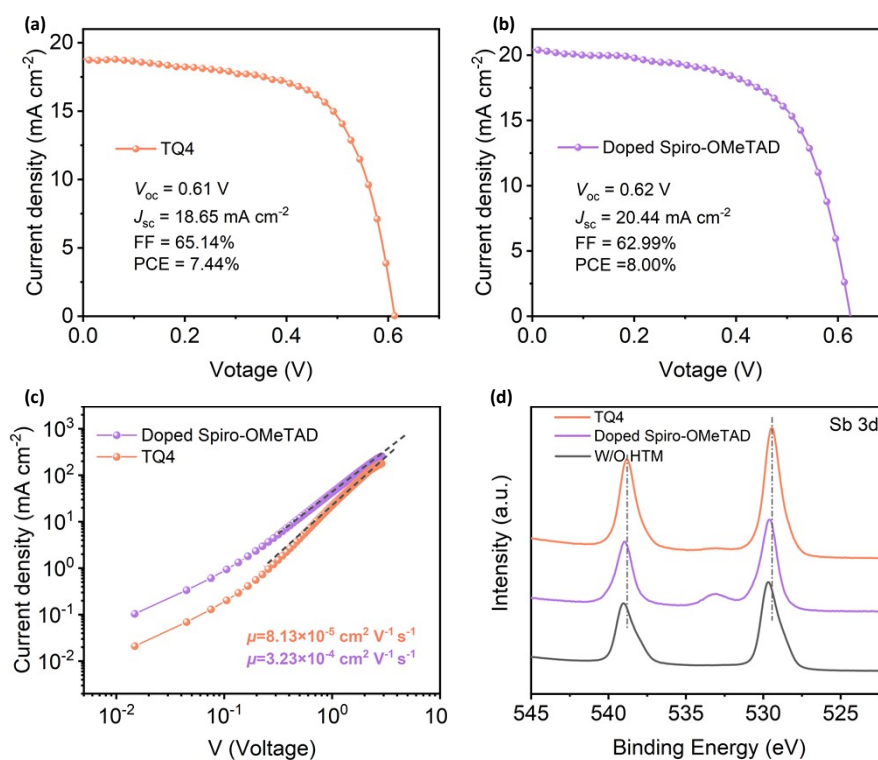


Figure S10 Current density-voltage (J-V) curves of (a) TQ4 and (b) doped Spiro-OMeTAD devices. (c) SCLC hole-mobility curves of devices with the structure of ITO/PEDOT:PSS/ TQ4 (ca. 30 nm) or doped Spiro-OMeTAD(ca. 50 nm)/MoO₃/Au. (d) XPS spectra of $\text{Sb}_2(\text{S,Se})_3$, $\text{Sb}_2(\text{S,Se})_3/\text{HTM}$ films for Sb element.

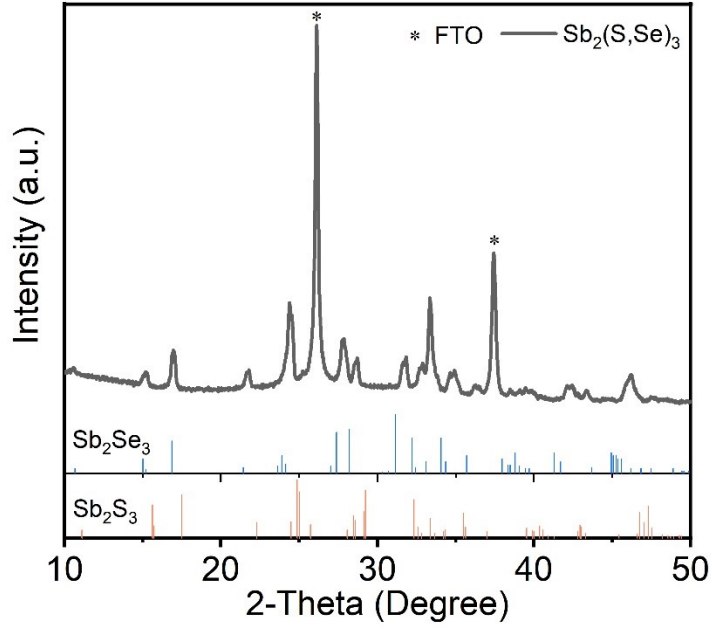


Figure S11 XRD pattern of the as-synthesized $\text{Sb}_2(\text{S,Se})_3$ film.

Table S1 Fitting results of TAS monitored at 620 nm wavelength

HTMs	A_1	$t_1(\text{ps})$	A_2	$t_2(\text{ps})$	$\tau(\text{ps})$
TQ2	0.25	261.81	0.75	4942.31	4861.23
TQ4	0.37	192.63	0.63	2895.00	2793.52

Table S2 Photovoltaic parameters of the control device and those with TQ2 and TQ4 as HTMs measured under 100 mW cm^{-2} solar simulator illumination

HTMs	V_{oc}/V	$J_{sc}/\text{mA}\cdot\text{cm}^{-2}$	FF	$\eta/\%$
TQ4	0.61 ± 0.01 (0.61)	18.37 ± 0.39 (18.82)	63.90 ± 1.66 (64.69)	7.16 ± 0.20 (7.46)
TQ2	0.61 ± 0.01 (0.61)	17.78 ± 0.49 (18.17)	57.12 ± 2.33 (58.74)	6.18 ± 0.23 (6.54)
W/O HTM	0.51 ± 0.03 (0.53)	16.14 ± 0.42 (16.44)	50.23 ± 0.25 (52.52)	4.11 ± 0.26 (4.55)

Note: The values in parentheses shows the parameters of the champion device.

Reference

1. H. Guo, H. Zhang, C. Shen, D. Zhang, S. Liu, Y. Wu and W. H. Zhu, *Angew Chem Int Ed Engl*, 2021, **60**, 2674-2679.
2. Y. Li, K. R. Scheel, R. G. Clevenger, W. Shou, H. Pan, K. V. Kilway and Z. Peng, *Advanced Energy Materials*, 2018, **8**.
3. M. Nikolka, K. Broch, J. Armitage, D. Hanifi, P. J. Nowack, D. Venkateshvaran, A. Sadhanala, J. Saska, M. Mascal, S. H. Jung, J. K. Lee, I. McCulloch, A. Salleo and H. Sirringhaus, *Nat Commun*, 2019, **10**, 2122.
4. G. Kresse and J. Furthmuller, *Phys. Rev. B*, 1996, **54**, 11169-11186.
5. G. Kresse and J. Hafner, *Phys Rev B Condens Matter*, 1993, **47**, 558-561.
6. S. Grimme, S. Ehrlich and L. Goerigk, *J Comput Chem*, 2011, **32**, 1456-1465.